

Ablation of Uroplakin III Gene Results in Small Urothelial Plaques, Urothelial Leakage, and Vesicoureteral Reflux

Ping Hu,^{*‡} Fang-Ming Deng,^{*} Feng-Xia Liang,^{*} Chuan-Min Hu,^{*} Anna B. Auerbach,[§] Ellen Shapiro,^{||} Xue-Ru Wu,^{||**} Bechara Kachar,^{‡‡} and Tung-Tien Sun^{*‡||}

^{*}Epithelial Biology Unit, The Ronald O. Perleman Department of Dermatology, [‡]Department of Pharmacology, [§]Skirball Institute of Biomolecular Medicine, ^{||}Department of Urology, and [¶]Department of Microbiology, Kaplan Comprehensive Cancer Center, New York University School of Medicine, New York, New York 10016; ^{**}Veterans Administration Medical Center, New York, New York 10010; and ^{‡‡}Section on Structural Cell Biology, National Institute on Deafness and Other Communication Disorders, National Institutes of Health, Bethesda, Maryland 20892

Abstract. Urothelium synthesizes a group of integral membrane proteins called uroplakins, which form two-dimensional crystals (urothelial plaques) covering >90% of the apical urothelial surface. We show that the ablation of the mouse uroplakin III (UPIII) gene leads to overexpression, defective glycosylation, and abnormal targeting of uroplakin Ib, the presumed partner of UPIII. The UPIII-depleted urothelium features small plaques, becomes leaky, and has enlarged ureteral orifices resulting in the back flow of urine, hydronephrosis, and altered renal function indicators. Thus, UPIII is an integral subunit of the urothelial plaque and contributes to the permeability barrier function of the urothelium, and UPIII deficiency can lead to global anomalies in the urinary tract. The ablation of a single urothelial-specific gene can therefore cause primary vesicoureteral

reflux (VUR), a hereditary disease affecting ~1% of pregnancies and representing a leading cause of renal failure in infants. The fact that VUR caused by UPIII deletion seems distinct from that caused by the deletion of angiotensin receptor II gene suggests the existence of VUR subtypes. Mutations in multiple gene, including some that are urothelial specific, may therefore cause different subtypes of primary reflux. Studies of VUR in animal models caused by well-defined genetic defects should lead to improved molecular classification, prenatal diagnosis, and therapy of this important hereditary problem.

Key words: urothelium • permeability • knockout mice • vesicoureteral reflux • hydronephrosis

Introduction

Urothelium, also known as transitional epithelium in older literature, lines almost the entire urinary tract including the renal pelvis, ureter, bladder, and proximal urethra (Hicks, 1975). Over 90% of the urothelial apical surface of the superficial umbrella cells is covered by rigid-appearing plaques (also known as asymmetric unit membranes) that are 0.2–0.5 μm in diameter (Porter and Bonneville, 1963; Hicks, 1965; Koss, 1969; Staehelin et al., 1972; Kachar et al., 1999). These plaques consist of two-dimensional crystalline arrays of hexagonally arranged 16-nm protein particles (Hicks and Ketterer, 1969; Vergara et al., 1969; Brisson and Wade, 1983; Walz et al., 1995; Kachar et al., 1999) that are composed of uroplakins—a group of integral membrane proteins synthesized by mammalian urothelia as their major differentiation products (Wu et al., 1990, 1994; Yu et al.,

1990, Sun et al., 1999). It has been suggested that these urothelial plaques: (a) stabilize the apical surface, thus preventing urothelial rupture during bladder distention (Staehelin et al., 1972); (b) regulate the apical surface area by their reversible retrieval from, and insertion into, the apical surface (Minsky and Chlapowski, 1978; Lewis and de Moura, 1982); and (c) contribute to the remarkable permeability barrier function of the urothelium (Hicks, 1975; Chang et al., 1994; Negrete et al., 1996). Thus far, four uroplakins (UP)¹ [i.e., UPIa (27 kD), UPIb (28 kD), UPII (15 kD), and UPIII (47 kD)], have been identified (Wu and Sun, 1993; Lin et al., 1994; Yu et al., 1994). The precise biological functions of the uroplakins, and the abnormalities that may be caused by uroplakin defects, are unknown.

Primary vesicoureteral reflux (VUR; OMIM, 1999), the retrograde flow of urine from the bladder into ureters and

Address correspondence to Tung-Tien Sun, Ph.D., Department of Dermatology, New York University Medical School, 550 First Avenue, New York, NY 10016. Tel.: (212) 263-5685. Fax: (212) 263-8561. E-mail: sunt01@med.nyu.edu

¹Abbreviations used in this paper: ES, embryonic stem; UP, uroplakin; VUR, vesicoureteral reflux.

kidneys, is hereditary as there is a 30–50-fold increased incidence of VUR in first degree relatives of such patients (Noe et al., 1992; Belman, 1997; Atala and Keating, 1998; Dillon and Goonasekera, 1998). VUR affects 0.5–1% of the population and is, therefore, one of the more common congenital abnormalities (Smellie and Normand, 1979; King, 1992; Becker and Avner, 1995; Belman, 1997; Atala and Keating, 1998; Dillon and Goonasekera, 1998; Hiraoaka et al., 1999; Horowitz et al., 1999). Infants or young children with VUR are highly susceptible to urinary tract infection. Reflux of infected urine into the kidneys can cause acute pyelonephritis and subsequent renal scarring, hypertension, and end-stage renal disease. Although VUR is the most common cause of renal failure in children, and an important cause in adults (Kincaid-Smith et al., 1984; Eccles et al., 1996), the genetic basis for VUR has not yet been clearly defined.

In this paper, we show that germline deletion of mouse uroplakin III gene resulted in the selective perturbation of its presumed partner, UPIb, and in the formation of a grossly abnormal urothelium devoid of a typical umbrella cell layer. The apical urothelial surface was covered with unusually small urothelial plaques interspersed by greatly expanded (particle-free) “hinge” areas, and the urothelium became leaky. Moreover, the mice had greatly enlarged ureteral orifices leading to vesicoureteral reflux, hydronephrosis, and altered renal function indicators. These results suggest that uroplakin III is an integral subunit of urothelial plaques that play a key role in urothelial structure and function, that urothelial defects can have global effects on the entire urinary system including the kidneys, and that mutations in a panel of urothelial-specific genes may play a role in human VUR.

Materials and Methods

Production of the UPIII Knockout Mice

Genomic clones of mouse UPIII gene were isolated from a 129/Ola mouse P1 genomic library (Genome Systems). The targeting vector, designed to delete exons 1–3 of the UPIII gene, contained four portions: a 5-kb *Ava*I mouse UPIII fragment upstream of exon 1, the neomycin-resistance gene driven by the phosphoglycerate kinase (PGK) promoter in the opposite direction, a 3-kb *Bam*HI mouse UPIII genomic fragment downstream of exon 3, and the thymidine kinase gene of herpes simplex virus driven by the PGK promoter (Joyner, 1993; Ramirez-Solis et al., 1993). The *Xho*I-linearized vector was electroporated into 129/SvEv embryonic stem cell line W4, and the Neo-positive and TK-negative transformants were selected using G418 (240 μ g/ml) and gancyclovir (2 μ M). 2 of 150 embryonic stem (ES) cell colonies were found to harbor the correct homologous recombination events as determined by Southern blotting using the “Probe” and by long-range PCR using primers LP1 and LP2 (Fig. 1 a, below). The confirmed ES cell clones were amplified and aggregated with eight cell-stage embryos of Swiss Webster mice, and implanted into pseudopregnant females. Five chimeric mice from two ES cell lines were germline-transmitting, and were bred with SW mice to yield hybrid homozygotes, or mated with 129/SvEv mice to yield inbred 129/SvEv UPIII-knockout mice.

RNA and Protein Analyses

Total RNA was isolated using RNagents System (Promega), separated on a 1% agarose/formaldehyde gel, and transferred to a Hybond-N membrane (Amersham Pharmacia Biotech). For Western blot analysis, total (SDS-solubilized) urothelial proteins from the equivalent of a quarter of a mouse bladder were separated on a 17% SDS-polyacrylamide gel, and transferred onto an MSI-nitrocellulose membrane (Fisher Scientific). The membrane was treated with 5% nonfat dry milk in PBS, and incubated

with an antibody. For immunohistochemistry, mouse tissues were fixed in 4% paraformaldehyde in PBS, paraffin-embedded, cut into 5- μ m sections, and immunostained using the peroxidase-antiperoxidase technique. Antibodies used in this study included: AE1 and AE3 mouse monoclonal antibodies to keratins (Tseng et al., 1982; Sun et al., 1984), rabbit antisera against synthetic peptides of individual uroplakins (Wu and Sun, 1993; Wu et al., 1994), and a mouse monoclonal antibody against uroplakin III (Riedel et al., 2000).

Electron Microscopy and Quick-Freeze/Deep Etch

For transmission electron microscopy, mouse bladder was cut into small pieces (<1 mm²), fixed with 2.5% glutaraldehyde in 0.1 M sodium cacodylate buffer, pH 7.4, post-fixed with 2% (wt/vol) osmium tetroxide, and embedded in Epon 812 (Polysciences, Inc.). For scanning EM, a bladder was bisected, fixed as above, and critical-point dried. For quick-freeze/deep etch, a fixed mouse bladder was cut into halves, rinsed with distilled water, and frozen to liquid nitrogen temperature using a Life Cell CF-100 freezing apparatus (Kachar et al., 1999; Liang et al., 1999).

Determination of the Micturition Pattern

The urination pattern was determined using a filter paper assay. 3-mo-old wild-type and UPIII-knockout mice were housed in a 12 h:12 h day/night cycled, germ-free animal facility. Mice were placed singly in a special cage fitted with a fine-meshed bottom, thus allowing the urine to land on a piece of filter paper, which could be changed periodically. Calibration studies established that the surface areas covered by the mouse urine, which was strongly fluorescent and thus could be easily visualized under a UV light, provided an accurate measurement of the urine volume (with a linear range of up to \sim 500 μ l).

Blood Urea Nitrogen and Serum Creatinine

Blood samples from mice (3-mo old) were drawn from the orbital sinus. Sera were prepared and the BUN and creatinine concentrations were measured by Antech Diagnostics.

Determination of Reflux Pressure and Dye Penetration

Mice (2–3-mo old) were anaesthetized by i.m. injection of a mixture of xylazine (10 mg/kg; Fort Dodge Animal Health) and ketamine (200 mg/kg; Bayer). The abdomens of the mice were surgically opened under a stereomicroscope to expose the urinary bladder. A 25-gauge butterfly needle (Fisher Scientific) was connected to a 5-ml syringe filled with a 0.1% rhodamine (Sigma-Aldrich) or an Indian Ink solution (10% vol/vol) in 0.9% NaCl, and was inserted into the bladder. The syringe was gradually raised at the rate of \sim 1 cm per min, and the hydrostatic pressure (cm-H₂O) at which urination or reflux occurred was recorded. If reflux did not occur even after urination, the urethral outlet was sealed by suture or by applying a drop of glue (Magic Glue). The experiment was then repeated to determine the pressure at which reflux occurred (at a pressure higher than micturition pressure). If vesicoureteral reflux did not occur at 90 cm-H₂O, the experiment was discontinued and the “vesicoureteral reflux pressure” was recorded as 90 cm-H₂O. For voiding cystoureterograms, iothalamate meglumine (Mallinckrodt Inc.) was infused into mouse bladder through a PE10 urethra catheter (0.28 mm i.d., 0.61 mm o.d.), and the animals were x rayed while the pressure was raised progressively.

For dye-leakage assays, mice were anaesthetized using xylazine/ketamine and catheterized using a PE10 tube. After the bladder was emptied by applying gentle pressure to the belly, 200 μ l of 0.1% methylene blue (Sigma-Aldrich) in 0.9% NaCl was instilled into the bladder (Fukui et al., 1983). The solution was removed 20 min later, and the bladder was washed with 3 ml of 0.9% NaCl solution. The bladder was extracted with 1 ml chloroform at 50°C overnight, and the OD 660 nm of the solvent was measured.

Results

Generation of Uroplakin III-depleted Mice

To ablate the mouse UPIII gene, we designed a targeting vector to delete its first three exons and to create a frame-shift mutation in its remaining exons (Fig. 1 a). The linearized vector was electroporated into W4 embryonic stem

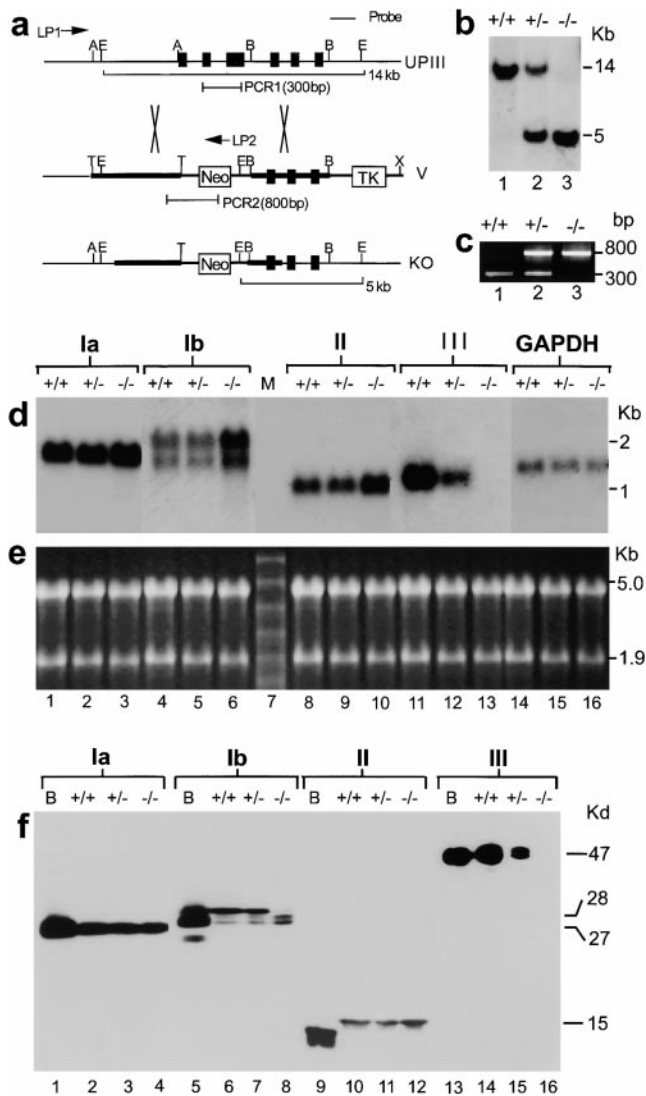


Figure 1. Ablation of *upk3* gene affected the expression of other uroplakins. (a) Alignment of the *upk3* locus, the targeting vector (V), and the mutated locus (KO). Solid boxes, exons; X, potential crossover site; probe, a genomic probe; LP1 and 2, long-template PCR primers; PCR1 and 2, PCR products characteristic of the wild-type and KO alleles, respectively; Neo, neomycin-resistant gene; TK, thymidine kinase of the herpes simplex virus; A, *Ava*I; B, *Bam*HI; E, *Eco*RI; T, *Taq*I; and X, *Xho*I. (b) Southern analysis of the *Eco*RI-digested mouse genomic DNA with the P probe that recognized 14- and 5-kb fragments from the wild-type and KO allele, respectively. +/+, wild type; +/-, heterozygote; and -/-, homozygote. (c) PCR analysis of the genomic DNA using a mixture of two pairs of primers that generated a 300- and an 800-bp product characteristic of the wild-type and KO allele, respectively. (d) Northern analysis. Total RNA samples (10 μ g) were resolved electrophoretically and probed with cDNA of mouse uroplakins Ia, Ib, II, and III, and glyceraldehyde phosphate dehydrogenase (GAPDH). Note the absence of UPIII message, and the $\sim 5\times$ increase in UPIb message in the -/- animal. (e) Ethidium bromide-stained rRNA of the samples in d as a loading control. M in lane 7 denotes RNA size markers. (f) Immunoblot analyses of mouse uroplakin proteins Ia (27 kD), Ib (28 kD), II (15 kD), and III (47 kD). Bovine total uroplakins (B) were included as a positive control. Note in the -/- mice the absence of UPIII, the roughly normal amounts of UPIa and UPII, and the absence of the major, slowest migrating UPIb species, possibly due to defective glycosylation.

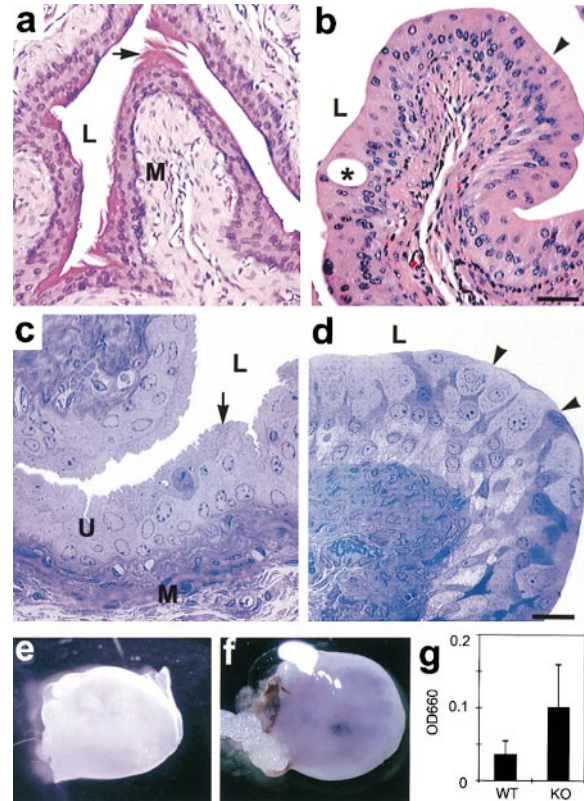


Figure 2. UPIII-depleted urothelium lacked the umbrella cells and was leaky. Normal (a, c, and e) and UPIII-depleted mouse bladders (b, d, and f), all from 2–3-mo-old mice, were examined using hematoxylin and eosin-stained paraffin sections (a and b), or using toluidine blue-stained plastic thin sections (c and d). Appearance of methylene blue-stained wild-type (e) and UPIII-knockout (f) mouse bladders. (g) Retention of methylene blue by wild-type ($n = 7$) and UPIII-depleted mouse ($n = 5$) bladder ($P = 0.019$). The dye that was retained by the bladder was solubilized with chloroform and read at 660 nm. Note the rugged luminal surface of the normal, superficial umbrella cells (arrows), and the markedly different UPIII-depleted urothelium, which was characterized by a smooth, apical cell surface (arrowheads), the absence of an umbrella cell layer, and the leakiness/retention of methylene blue. L, bladder lumen; M, mesenchyme; and U, urothelium. Bars: 50 μ m (a and b) and 25 μ m (c and d).

cells, and the neo- and gancyclovir-resistant cells were selected. Two ES cell colonies (C1 and C2) harbored the desired recombination events according to PCR and Southern blot analysis (data not shown), and gave rise to germline-transmitting chimeric mice. Five male chimeras (four C1 and one C2) carrying the mutated UPIII gene were crossed with SW (or 129/SvEv) females to generate F1 heterozygotes, which were then bred to produce the F2 hybrids, with the mutated UPIII allele segregating in a Mendelian fashion (Fig. 1, b and c). Since similar results were obtained from the offspring of the two ES clones, six UPIII (-/-) breeding pairs from C1 were used to produce homozygous F2 (-/-) mice. Two of the pairs yielded offspring that were small and most of them died 10–14 d postnatally (see below). The other four pairs produced UPIII (-/-) offspring that showed consistent and well-defined urinary tract defects; these animals, which grew and reproduced relatively normally, were characterized in detail and reported here.

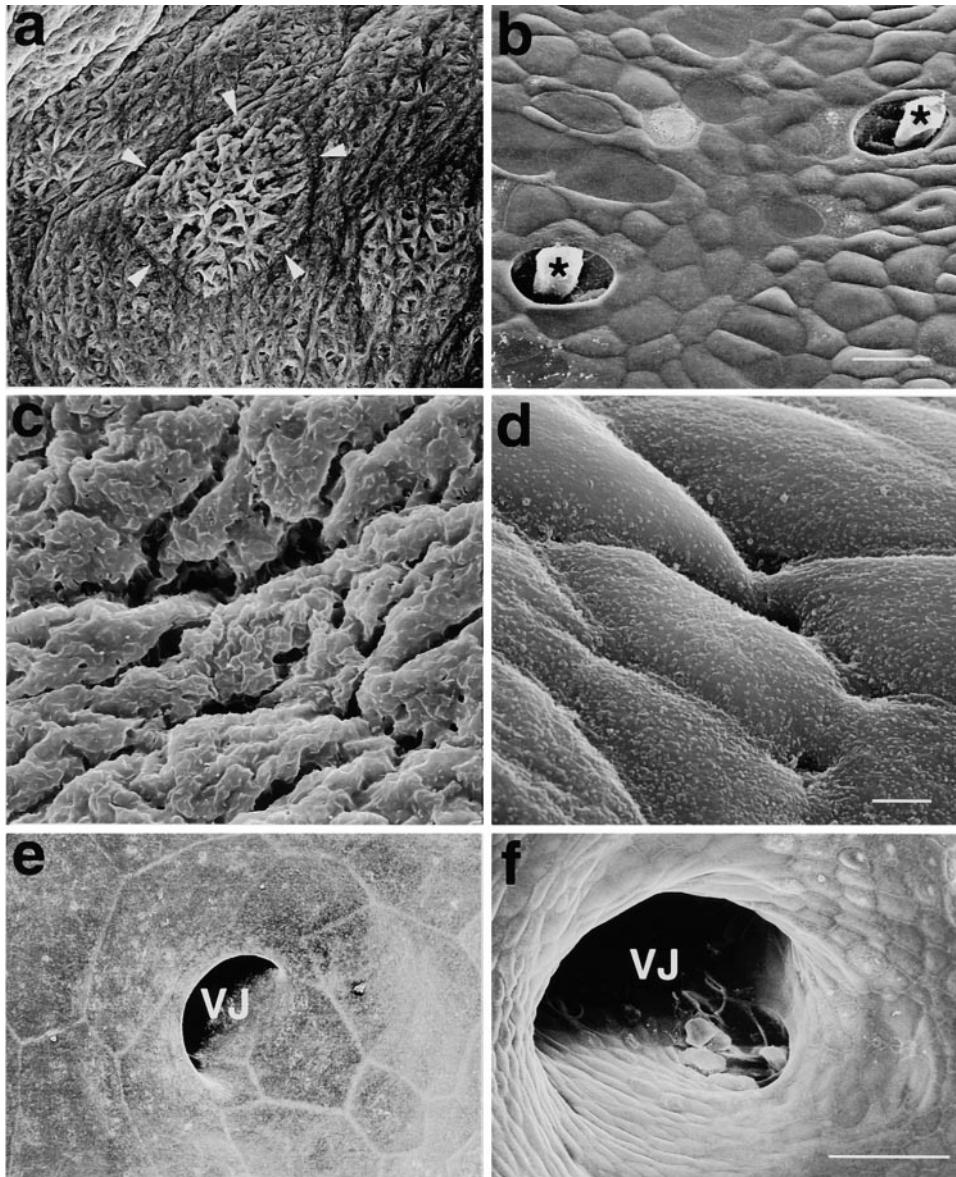


Figure 3. UPIII-depleted mice had altered urothelial apical surface and enlarged ureteral orifices. The apical surfaces of normal (a, c, and e) and UPIII-depleted (b, d, and f) urothelia (of 2–3-mo-old mice) were examined by scanning EM. Note the highly rugged and folded surface of large (~100–150- μm diameter) normal umbrella cells (arrowheads mark the outline of one such cell in a) and the much smaller (15–25 μm) and smooth surfaced, UPIII-depleted superficial cells. Also note the frequent desquamation of the superficial cells (b, *) and the much larger ureteral orifice (vesicoureteral junction, VJ; 120–150- vs. 40–60- μm diameter) of the UPIII-depleted bladder. Bars: 25 μm (a and b), 5 μm (c and d), and 50 μm (e and f).

Perturbed Uroplakin Expression and Grossly Abnormal Urothelial Apical Surface

The homozygous mice lacked UPIII message (Fig. 1 d, lane 13) and protein (f, lane 16), thus confirming the ablation of UPIII gene. The heterozygotes had a reduced amount of UPIII, suggesting a gene dosage effect (Fig. 1 d, lane 12, and f, lane 15). The mRNA level of UPIb, which we previously suggested pairs with UPIII (Wu et al., 1995), was elevated approximately fivefold (Fig. 1 d, lane 6), while those of UPIa (lane 3) and UPII (lane 10) increased only approximately twofold. On the protein level, while the migration patterns of UPIa and II were normal (Fig. 1 f, lanes 4 and 12), UPIb was altered in that its major, highest molecular weight species was missing, suggesting incomplete glycosylation (lane 8) (Yu et al., 1994). Taken together, these results clearly established the elimination of UPIII in the homozygous ($-/-$) mice, and indicated that UPIII ablation affected more the synthesis and processing of UPIb, its presumed partner (Wu et al., 1995), than those of UPIa and UPII (also see below).

While normal mouse urothelium was relatively thin, consisting of three to four nuclear tiers with a characteristic, superficial “umbrella” cell layer (Fig. 2, a and c), the UPIII-depleted urothelium was almost twice as thick due to an increase in nuclear tiers four to five, as well as a change of the superficial squamous cells to become cuboidal or even columnar (Fig. 2, b and d). We then examined the ultrastructure of these altered superficial cells, which no longer possessed a typical umbrella cell layer (Fig. 2, b and d), by scanning and transmission electron microscopy, as well as by the quick-freeze deep-etch technique (Figs. 3 and 4). Normal umbrella cells could be as large as 150 μm in diameter (Fig. 3, a and e), their cytoplasm was filled with uroplakin-delivering fusiform vesicles (Fig. 4 a), and they had a rugged apical surface due to the presence of numerous plaques (Figs. 3, a and c, and 4 a) consisting of 16-nm particles hexagonally arranged forming two-dimensional crystals (average 1,400–3,000 particles per plaque; Fig. 4 c) that covered ~90% of the apical cell surface area (Porter and Bonneville, 1963; Hicks, 1965; Koss, 1969; Surya et al., 1990; Walz et al., 1995; Kachar et al., 1999). In contrast, the

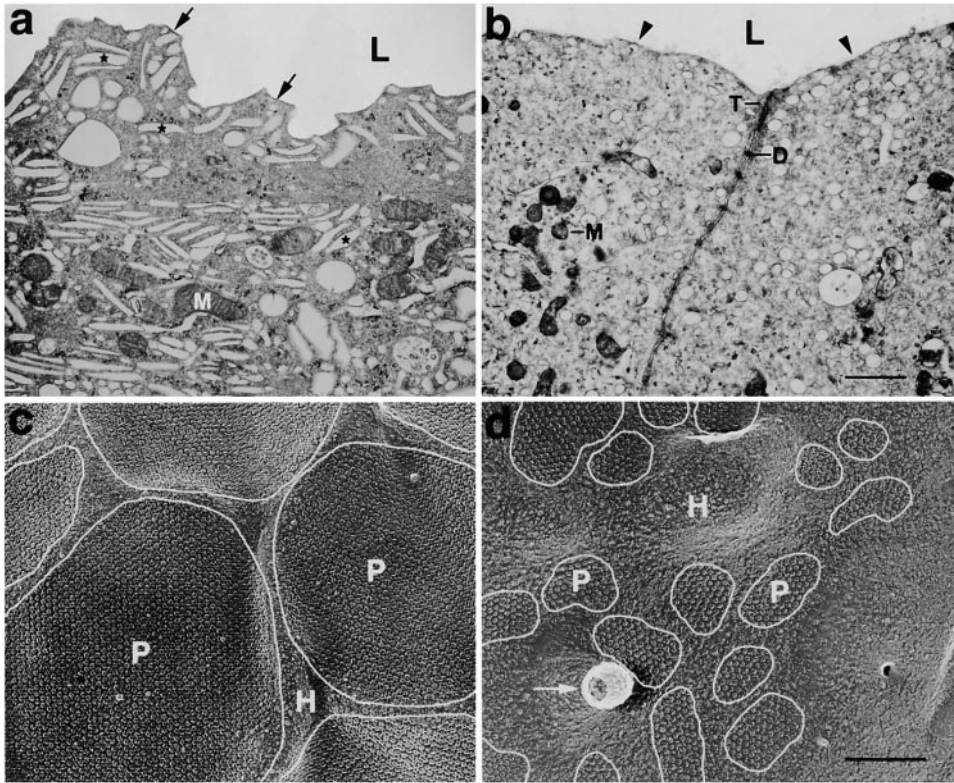


Figure 4. UPIII-negative urothelium lacked the uroplakin-containing fusiform vesicles and the normal, apical urothelial plaques. Normal (left) and UPIII-depleted (right) mouse bladder (of 2–3-mo-old mice) were examined by transmission electron microscopy (a and b) and by quick-freeze/deep etch (c and d). Note in normal urothelium the abundant (uroplakin-delivering) fusiform cytoplasmic vesicles (a, *), and the large plaques (a, arrows) consisting of two-dimensional crystals of hexagonally arranged 16-nm uroplakin protein particles (c, plaque or P), which covered almost the entire urothelial

apical surface. In contrast, note in the uroplakin III-negative urothelium the accumulation of immature, discoidal, cytoplasmic vesicles and the absence of mature, fusiform vesicles, the relatively smooth apical surface (arrowheads) with occasional pleomorphic microvilli (d, arrow), and the conspicuously small urothelial plaques (P) and the wide interplaque space (hinge or H). D, L, M, and T denote desmosome, lumen, mitochondria, and tight junction, respectively. Bars: 1,000 nm (a and b) and 200 nm (c and d).

apical cells of UPIII-depleted urothelium were only 15–25 μm in diameter and were frequently seen to contract and detach (Fig. 3, b and f), their cytoplasm lacked the mature fusiform vesicles that were replaced by immature, smaller discoidal vesicles (Fig. 4 b), and their apical surface was relatively smooth (Figs. 3, b and d, and 4 b) with abnormally small crystalline plaques (40–150 particles per plaque) interspersed by wide, particle-free hinge areas (Fig. 4, c and d). Fourier transformation of the small plaques of the knockout urothelium revealed the same hexagonal symmetry and 16-nm center-to-center distance between neighboring particles. Consistent with the decrease in the surface area covered by urothelial plaques, which have been suggested to play a role as a permeability barrier (Chang et al., 1994), the UPIII-depleted bladder was leaky to methylene blue (Fig. 2, e–g) (Fukui et al., 1983). The mesenchymal tissue immediately underneath the urothelium was slightly more cellular with occasional inflammatory cells when compared with the controls (Fig. 2, b and d; data not shown).

UPIII Ablation Led to Altered Targeting of Its Partner UPIb

To localize the uroplakins, we immunohistochemically stained the normal and UPIII-depleted mouse urothelia using antibodies monospecific for the four uroplakins (Fig. 5). Uroplakin staining was seen in all suprabasal cell layers of the normal urothelium (Fig. 5, left). Particularly intense staining of the apical urothelial surface by all four uroplakin antibodies was evident, consistent with the fact that

the apical surface is highly enriched with urothelial plaques (Fig. 5, left). The uroplakin expression pattern of the UPIII-depleted urothelium was significantly altered (Fig. 5, right). No UPIII could be detected (Fig. 5 d), thus confirming the Northern and immunoblotting data (Fig. 1, d and f). Although the UPIII-depleted urothelium showed strong anti-keratin staining (Fig. 5 b), its staining intensity with antibodies to uroplakins Ia, Ib, and II was in general reduced. Interestingly, although UPIa and UPII still showed a typical enrichment at the apical cell surface (Fig. 5, f and j; arrowheads), UPIb (the putative partner of UPIII) showed only weak, diffuse cytoplasmic and basal-lateral cell periphery staining, without apical enrichment (Fig. 5 h, *). These results indicated that the elimination of UPIII selectively affected the expression and targeting of its presumed partner, UPIb (Wu et al., 1995).

Uroplakin III Deficiency and Vesicoureteral Reflux

Another striking feature of the UPIII-depleted mice ($n = 5$) was that their ureteral orifices were greatly enlarged (120–150 μm instead of the usual 40–60 μm diameter, wild-type mice, $n = 4$; Fig. 3, e and f). Since enlarged ureteral orifice is thought to be an underlying feature of primary VUR (Ambrose, 1969; Lyon et al., 1969), we instilled an Indian Ink solution (via a needle) into the exposed bladders of anesthetized mice and measured the hydrostatic pressure at which urine began to back flow into the ureters (Fig. 6, a and b). The micturition pressure (the hydrostatic pressure that induced urination) of the UPIII-depleted mice was ~ 30 cm

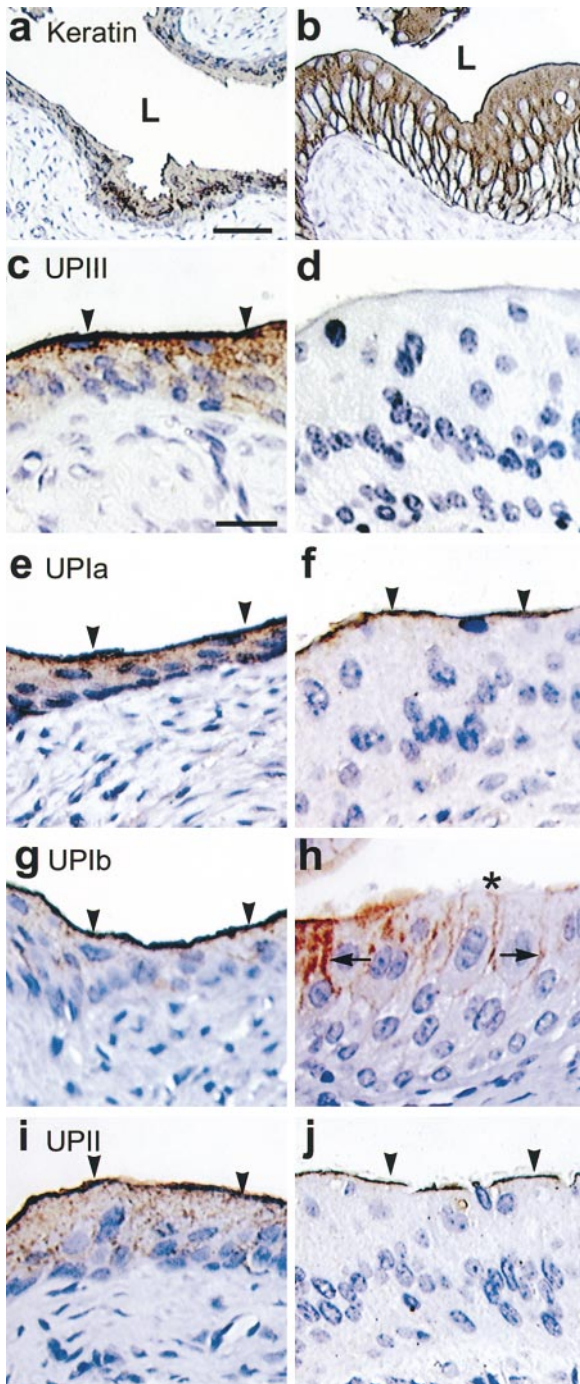


Figure 5. Altered expression of uroplakins in the UPIII-depleted urothelium. Paraffin-sections of normal (left) and uroplakin III-depleted (2–3-mo-old) mouse urothelia (right) were deparaffinized and stained immunohistochemically using antibodies to keratins (AE1 plus AE3) (a and b), uroplakin III (c and d), uroplakin Ia (e and f), uroplakin Ib (g and h), and uroplakin II (i and j). Note the concentration of all four uroplakins on the apical surface of normal urothelium (arrowheads); in contrast, only UPIa and UPII are apical-concentrated in the UPIII-depleted urothelium. (h, arrows) The association of UPIb with lateral cell surface, instead of apical surface (*) of the UPIII-depleted urothelium. L, bladder lumen. Bars: 25 μ m (a and b) and 50 μ m (c–j).

H₂O, which was about the same as those of the two parental mouse strains (SW and 129/SvEv) and their wild-type siblings (Fig. 6 c). The reflux pressure of the parental strains as well as the unaffected siblings was >50 cm-H₂O; this was an

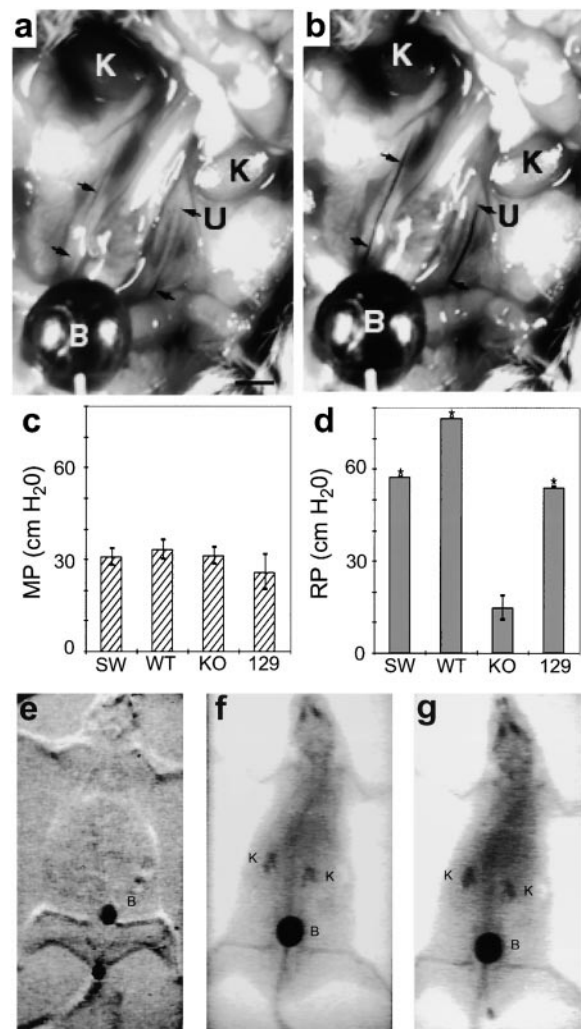


Figure 6. UPIII-depleted mice had vesicoureteral reflux (VUR). (a–b) An Indian Ink assay. Instillation of a 0.1% Indian Ink solution into the bladders of the UPIII-depleted mice (2–3-mo old) at hydrostatic pressures of 10 (a) and 26 (b) mm-H₂O. This animal had reflux and micturition pressures of 15 and 28.5 cm-H₂O, respectively. Note the retrograde flow of the black fluid into the ureters in (b). (c) The micturition pressure was measured for the two parent mouse strains; i.e., SW ($n = 10$) and 129/SvEv ($n = 7$), as well as the UPIII-knock-out (KO) mice ($n = 5$) and their wild-type (WT) siblings ($n = 5$). Note that all four mouse strains had about the same micturition pressure (MP) of 25–30 cm-H₂O. (d) The vesicoureteral reflux pressure (RP) of the same four mouse lines. Note the occurrence of vesicoureteral reflux in the UPIII-depleted mice at \sim 15 cm-H₂O, which was significantly lower than the other three control strains (>55 cm; $P = 0.005$). Brackets indicate SD. *The RP of animals that did not reflux at 90 cm-H₂O were arbitrarily taken as 90; thus the RP of SW, WT, and 129 were greatly underestimated. (e and f) Voiding cystoureterogram of normal animal showing no reflux (e) and of a UPIII-KO mouse showing reflux into the kidneys (f and g). B, bladder; K, kidney; and U, ureter. Bars: 5 mm (a and b).

under-estimation because many of the control mice could not be induced to reflux even when the hydrostatic pressure was raised to >90 cm-H₂O (Fig. 6 d). Some of the normal mice refluxed briefly during urination, probably reflecting a transient, high voiding pressure. In contrast, all the UPIII (–/–) mice refluxed at an extremely low pressure of 14.8 ± 3.9 cm-H₂O ($P = 0.005$; Fig. 6 d). The reflux was confirmed by a voiding cystoureterogram (Fig. 6, e–g), a standard pro-

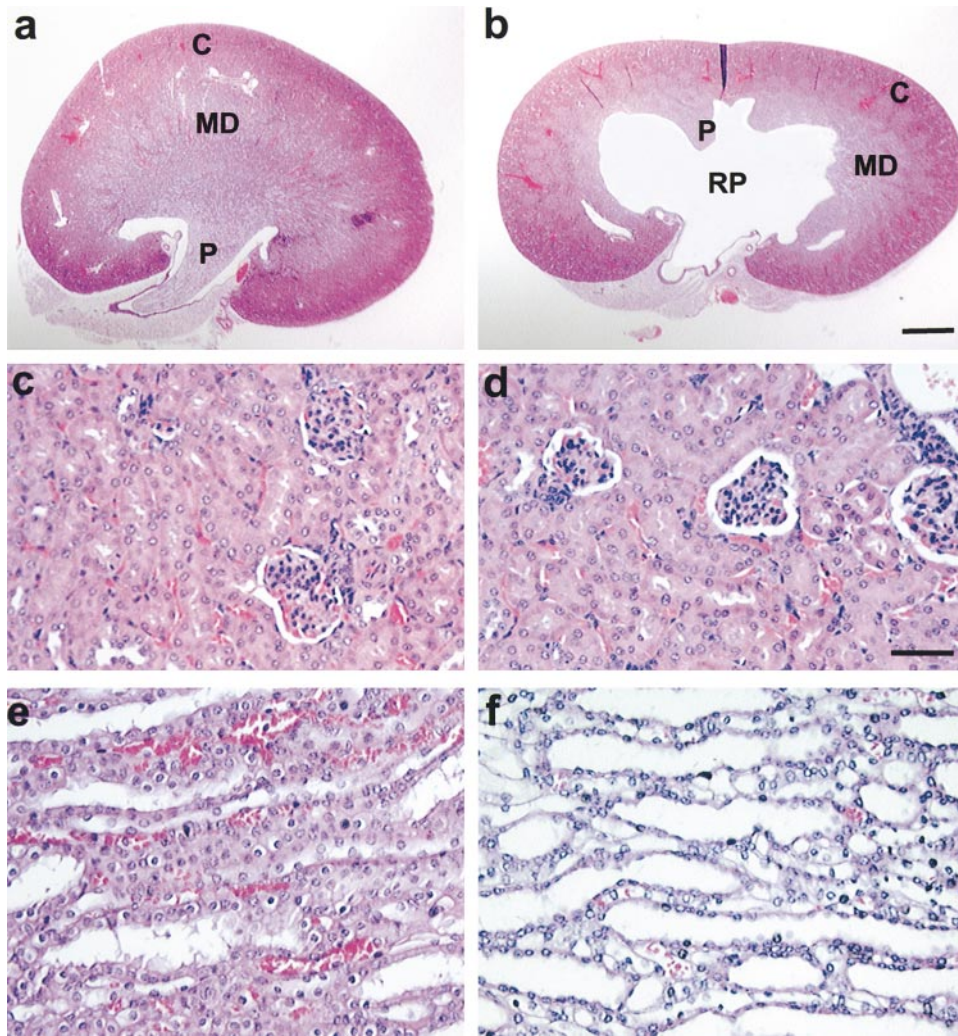


Figure 7. UPIII-ablation induced hydronephrosis and kidney abnormalities. Paraffin sections (hematoxylin and eosin stained) of kidneys of normal (a, c, and e) and UPIII-depleted (b, d, and f) mice (2–3-mo old). (a and b) Low magnification view, (c and d) cortex, and (e and f) papilla. Note the expanded renal pelvic space and the dilation of the collecting ducts in the UPIII-depleted mice. C, cortex; MD, medulla; P, papilla; and RP, renal pelvis. Bar: 1 mm (a and b) and 50 μ m (e and f).

cedure for diagnosing VUR in humans. These results clearly established that our UPIII-depleted mice had abnormal ureteral orifices and VUR.

Hydronephrosis and Altered Renal Function Indicators

Since it is known that reflux can sometimes lead to renal damage and nephropathy, we assessed the renal structure and function of the UPIII-depleted mice. The renal pelvis of many such mice was enlarged ($n = 12$ of 20 F1 UPIII-deficient animals; Fig. 7, a and b), with significantly dilated collecting ducts and distal tubules (e and f), but minimally perturbed renal cortex (c and d). To assess the micturition pattern, we housed the mice singly in (fine) wire-floored cages underlined with a filter paper that was changed at regular intervals, so that the urine volume could be measured based on the surface areas covered by the fluorescent urine (Fig. 8 a). We found that while the average volume per micturition of the UPIII-depleted mice was within the normal range (Fig. 8 b), the UPIII-depleted mice urinated almost twice as frequently as the controls ($P = 0.009$; Fig. 8 c), resulting in a doubling of the total urine output per day ($P = 0.008$; Fig. 8 d). Moreover, unlike the normal urine that had a pH value of 5–7 ($n = 30$), the urinary pH of $\sim 15\%$ of the knockout mice ($n = 45$) was ≥ 8 . Finally, the levels of serum creatinine and blood urea nitrogen of the UPIII-depleted mice were 1.36 ($P = 0.05$) and 1.4 ($P = 0.01$) times higher than those of the control

animals (Fig. 8, e and f). Similar results were obtained with male and female animals (Fig. 8, b–d). These results indicated that some of the indicators of renal function, including filtration, concentration, and urine acidification, had been affected. Although these changes could reflect renal damage or dysfunction, it is also possible that they simply reflect the reabsorption of some of the urine components through a leaky urothelium.

Discussion

Using the gene-targeting approach, we show here that uroplakin III plays an indispensable role in forming normal urothelial plaques, that UPIII pairs with UPIb, that UPIII deficiency perturbs important urothelial functions, and that this deficiency can lead to VUR and associated anomalies affecting the entire urinary system, including the kidneys.

Uroplakin III Deficiency Causes Major Urothelial Anomalies

Numerous examples exist in which mutations in a tissue-specific differentiation product lead to organ-restricted abnormalities. We therefore sought to determine whether defects in uroplakins, the major differentiation products of urothelium, would cause urothelial-specific problems. Two issues were of concern, however, in taking this approach. First, although urothelial research has been tradi-

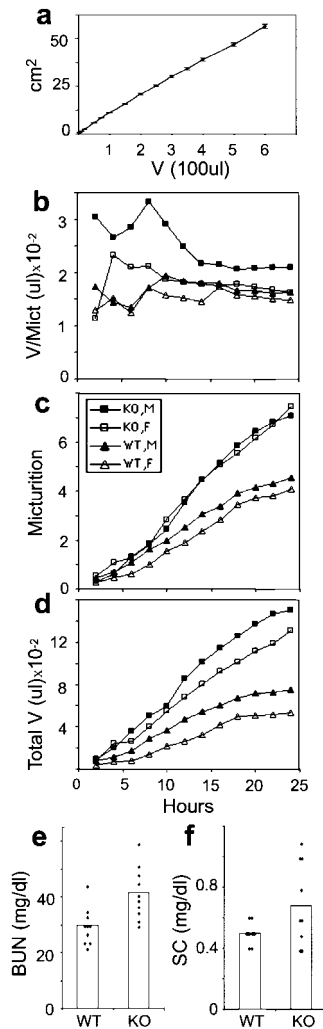


Figure 8. Renal function of the UPIII-depleted mice. The micturition pattern of UPIII-depleted mice (13 males and 11 females, all 2–3-mo old) and an equal number of their wild-type siblings were determined by measuring the surface area of a filter paper that was covered by the fluorescent urine (see Materials and Methods); the paper was changed every 15 min during a period of 24 h. (a) The standard curve showing the correlation between the mouse urine volume and the surface area covered by the fluorescent urine. (b) Average volume (V; μ l) of urine per micturition. (c) Number of micturition (times). (d) The cumulative urine volume. For blood analysis, sera from 10 UPIII-depleted and 10 wild-type sibling mice were pooled. (e) Blood urea nitrogen (BUN) concentration of the wild-type and UPIII-knockout mice. (f) Serum creatinine (SC) concentration of the wild-type and knockout mice.

tionally focused on the bladder, no known congenital bladder disease other than exstrophy (Shapiro et al., 1984) exists in the literature. Second, sequence analysis indicates that the four uroplakins can be divided into two structurally related groups. Thus, UPIa and UPIb are closely related, sharing \sim 30% of their amino acid sequence, and both belong to a family of proteins, called tetraspanins, having four transmembrane domains (TMD) (Yu et al., 1994). On the other hand, UPII and UPIII have only one TMD, and they share a stretch of \sim 12 amino acids that are adjacent to the TMD on the NH₂-terminal, luminal side (Wu and Sun, 1993; Lin et al., 1994). It is possible, therefore, that the structurally related UPII and UPIII (or UPIa and Ib) can substitute for its defective “analogue,” resulting in no phenotype. Such a functional redundancy could explain why no congenital bladder disease seems to exist.

Our data clearly demonstrate, however, that UPIII cannot be substituted by its structurally related UPII (Figs. 2–8). This is perhaps not surprising, given the limited structural similarity between these two proteins and the fact that UPIII has several unique features. First, UPIII is the only uroplakin possessing a significant cytoplasmic domain (of \sim 50 amino acids) that may play a role in anchoring the urothelial plaques onto an underlying cytoskeleton (Staelin et al., 1972; Wu and Sun, 1993). Second, while UPIa and UPIb harbor only 1–2-kD equivalents of high mannose sugars and the mature UPII harbors no sugars, uroplakin

III harbors almost 20-kD equivalents of complex sugars (Wu and Sun, 1993). UPIII may therefore contribute to most of the sugar components present on the apical surface of urothelial plaques. Third, chemical cross-linking studies have shown that uroplakins III and II bind preferentially to uroplakins Ib and Ia, respectively (Wu et al., 1995). Despite the structural similarities between UPIa and Ib, we show here that UPIII deletion selectively affects UPIb expression and maturation (Figs. 1 and 5). This, plus the specific interaction of UPIa and Ib with UPII and III, respectively, strongly suggests that even the structurally closely related UPIa and Ib are functionally distinct *in vivo*.

We have thus provided the first animal model of congenital urinary tract anomalies due to urothelial defects, in this case caused by the deletion of uroplakin III gene. In addition, the fact that uroplakins may not be functionally redundant greatly increases the likelihood that mutations in UPIII and other uroplakins can cause urothelial defects resulting in extensive abnormalities in the entire urinary tract—a concept that can have major clinical implications (see below).

Roles of UPIII and Uroplakin Pairs in Urothelial Plaque Formation

Based on the fact that uroplakins are the main protein components found in highly purified mammalian urothelial plaques, and also based on immunogold localization data, we suggested previously that uroplakins are the major building blocks of urothelial plaques (Wu et al., 1990; Yu et al., 1990). Furthermore, as mentioned, cross-linking studies suggested the existence of two uroplakin pairs (Wu et al., 1995). Our present data confirm and extend these observations. (a) Knockout of UPIII results in a grossly reduced number of apical urothelial plaques (Fig. 4), thus providing unequivocal proof that UPIII is an integral subunit of the plaques. (b) At the messenger RNA level, although UPIII-knockout does not significantly alter the level of uroplakins Ia and II mRNA’s (approximately two-fold), it induces an approximately fivefold increase in UPIb message, possibly due to a feedback regulation (Fig. 1 d). (c) At the protein level, UPIII deletion does not appreciably alter the amounts of UPIa and UPII (Fig. 1 f); however, this hampers UPIb maturation, suggesting that specific interactions between UPIb and III, presumably occurring in the rough endoplasmic reticulum, play a crucial role in UPIb maturation (Fig. 1 f) (Wu et al., 1995). (d) Immunohistochemical staining of the UPIII-negative urothelium shows that only uroplakins Ia and II are concentrated on the apical urothelial surface, while (the partnerless) UPIb is distributed diffusely in the cytoplasm and in the basal/lateral cell periphery (Fig. 5). (e) Only small patches of the urothelial plaque remain on the apical surface of the UPIII-negative urothelium (Fig. 4 d); such small patches have structural parameters similar to the normal plaques and are likely to consist of the Ia/II uroplakins.

Taken together, these data indicate that deletion of UPIII leads to the abnormal maturation of its partner UPIb (Figs. 1 and 5), thus providing strong support to the concept that the four known uroplakins form two pairs consisting of uroplakins Ia/II and Ib/III (Figs. 1 and 5), and that the remaining Ia/II pair can only form abnormally small patches of urothelial plaques (Fig. 4). These results provide unambiguous evidence that UPIII is an integral and indispensable subunit of urothelial plaques, which are

required for maintaining a normal-looking and functionally competent urothelium (Figs. 2–4). Further analysis of the UPIII-depleted mice should provide excellent opportunities to define more precisely the functional role of urothelial plaques in establishing the permeability barrier and other properties of the urothelium. Results from such analyses can also have implications for certain bladder diseases, such as interstitial cystitis.

Functional Roles of Urothelial Plaques

As the major specialization product of mammalian urothelia, the apical surface plaques are thought to perform three possible functions that are not necessarily mutually exclusive, including physical stabilization, surface area adjustment, and permeability barrier. Although the plaques of the UPIII-depleted urothelium are unusually small and widely dispersed (Fig. 4 d), careful histological examination of the urothelia from >20 adult animals revealed no evidence of urothelial rupture. In addition, the average micturition volume of the UPIII-depleted mice is normal, indicating that if the smaller plaques have hampered the reversible adjustment of urothelial surface area, such a defect has not resulted in a significantly diminished bladder capacity (Fig. 8 b). Interestingly, although normal urothelium is impermeable to methylene blue, this dye readily penetrates the UPIII-depleted urothelium (Fig. 2, e–g) and is taken up by the nuclei, suggesting that the dye has entered the urothelial cell via its apical surface. A compromised permeability barrier function may explain some of the phenotypes of the UPIII-depleted mice. It is known that if, during development, Wolffian duct budding occurs too close to the future bladder, this can lead to the displacement of the vesicoureteral junction to a more lateral region of the bladder, resulting in a shortened intravesical ureteral tunnel with an enlarged orifice (Atala and Keating, 1998; Pope et al., 1999). It is possible that the defective urothelium somehow perturbs this budding process, resulting in enlarged ureteral orifices and the subsequent vesicoureteral reflux, hydronephrosis, and altered renal function. Overall, although one cannot exclude the roles of stabilization and surface area adjustment, our data strongly support the idea that urothelial plaques contribute to the permeability barrier function (Hicks, 1975; Chang et al., 1994). Additional studies are underway to better define the electric resistance and permeability parameters of the UPIII-depleted urothelium.

Interstitial cystitis, the “painful bladder syndrome” affecting mainly women, is characterized by pelvic and/or perineal pain, urinary urgency, and frequency (Sant and Theoharides, 1999). It has been suggested that defects in the urothelial permeability barrier may allow some urine components to leak into the underlying mesenchymal tissues, causing irritation and inflammation, which, in turn, lead to some of the above symptoms. It is interesting to note that the UPIII-depleted mice have a rather normal urine volume per micturition (Fig. 8 b), suggesting that urothelial leakage (Fig. 2, e–g) may not necessarily lead to irritation-related urinary urgency, as indicated by a reduced volume per micturition.

Urothelial Defects May Cause a Subgroup of Human VUR

Although VUR is thought to facilitate urinary tract infection, it has also been suggested that it is infection, with the

release of bacterial endotoxins, that inhibits ureteral peristalsis, thus causing vesicoureteral reflux (Roberts, 1992; Garin et al., 1998). However, our experiments clearly demonstrate that VUR can occur as a primary event. This interpretation is consistent with the clinical finding that although 38% of pediatric patients with urinary tract infection have vesicoureteral reflux, a remarkable 48% of the asymptomatic siblings of these patients were also found to have reflux (Peeden and Noe, 1992).

Conflicting data exist regarding the hereditary basis of VUR. Thus, it has been proposed that VUR involves the dominant negative mutations of a single gene (Bailey et al., 1984; Chapman et al., 1985), but it has also been said that VUR is polygenic and heterogeneous with incomplete penetrance (de Vargas et al., 1978; Nishimura et al., 1999; Feather et al., 2000). Moreover, since VUR is sometimes associated with other congenital uropathies and nephropathies including ureteral duplication, vesicoureteral junction obstruction, ureteropelvic junction obstruction, and renal aplasia, hypoplasia and dysplasia, it has been suggested that VUR and some of these other urological and renal malformations share common mutations (Atwell, 1985; Becker and Avner, 1995; Devriendt et al., 1998; Pope et al., 1999). In this regard, it is interesting that the deletion of the angiotensin type 2 receptor gene (AGTR2) can also cause VUR. However, the VUR of the AGTR2- and UPIII-depleted mice seems to be different. Thus, the AGTR2 deletion-induced VUR affects only a small percentage of male mice with low penetrance and is associated with other forms of congenital anomalies of the kidney and urinary tract (CAKUT) (Nishimura et al., 1999). On the other hand, the UPIII depletion-induced VUR affects both sexes equally with high penetrance and it occurs in the absence of other forms of CAKUT. These results strongly suggest that there are at least two subtypes of VUR with distinct genetic bases.

We have shown here that the ablation of uroplakin III gene can cause VUR, and it will be of major interest to see whether defects in several other urothelial-specific genes will yield similar or related phenotypes. Like UPIII, these genes are expressed as terminal differentiation markers and are associated with the umbrella cells; they include uroplakins Ia, Ib, and II (Wu and Sun, 1993; Lin et al., 1994; Yu et al., 1994; Sun et al., 1999), and an 85-kD urohingin (Yu et al., 1992). The urothelium specificity of these genes makes them good candidate genes that can cause multiple anomalies within the urinary tract. That some of these genes may be involved in human VUR is suggested by a recent report that mapped VUR genes to multiple chromosomal sites, including two that coincide with the location of genes encoding uroplakin III (chromosome 22, 40–44 cM) and uroplakin Ib (chromosome 3, 117–184 cM) (Finch et al., 1997; Feather et al., 2000). Additional studies are needed to determine whether defects in such genes are indeed involved in subpopulation of human VUR.

Concluding Remarks

Studies on the uroplakin III-knockout mice that we describe here have shed light on the structure and function of urothelial plaques and on the possible molecular bases of VUR. Our results also raise several important questions. How are the uroplakins targeted and assembled at the urothelial apical surface? What is the role of the genetic

background in affecting the severity of the disease phenotype? What are the developmental pathways of VUR formation? What is the role of nontrauma-induced reflux in the pyelonephritis that occurs frequently in reflux patients? Finally, will the compromised urothelial permeability barrier function, coupled with other factors, lead to a hyperactive or hypersensitive bladder, and/or enhanced bladder tumorigenesis? Additional studies on mouse model systems, such as the one described here, should allow us to address these important issues.

We thank Alexandra Joyner for her substantial guidance and help in generating the knockout mice, Edith Robbins and David Sabatini for their generous help with scanning electron microscopy, Nancy Genieser and Peter K. Nelson for performing the voiding cystoureterogram, the Interstitial Cystitis Association, Bladder Foundation and New York University Urology Research Program for support, Xiangpeng Kong, Gert Kreibich, Pablo A. Morales, Angel Pellicer, Vicki Ratner, Robert Schacht and Mark Zeidel for useful discussions, and Herbert Lepor and Irwin M. Freedberg for encouragement and support.

This work was funded by National Institutes of Health grants DK39753, DK52206, and DK57269.

Submitted: 11 August 2000

Revised: 9 October 2000

Accepted: 11 October 2000

References

Ambrose, S.S. 1969. Reflux pyelonephritis in adults secondary to congenital lesions of the ureteral orifice. *J. Urol.* 102:302–304.

Atala, A.A., and M.A. Keating. 1998. Vesicoureteral reflux and megaureter. In *Campbell's Urology*. P.C. Walsh, A.B. Retik, E.D. Vaughan, Jr., and A.J. Wein, editors. W.B. Saunders & Co., Philadelphia, PA. 1859–1917.

Atwell, J.D. 1985. Familial pelviureteric junction hydronephrosis and its association with a duplex pelviccalyceal system and vesicoureteric reflux. A family study. *Br. J. Urol.* 57:365–369.

Bailey, R.R., E. Janus, K. McLoughlin, K.L. Lynn, and G.D. Abbott. 1984. Familial and genetic data in reflux nephropathy. In *Reflux Nephropathy Update*. C.J. Hodson, R.H. Heptinstall, and J. Winberg, editors. Karger AG, Basel, Switzerland. 40–51.

Becker, N., and E.D. Avner. 1995. Congenital nephropathies and uropathies. *Pediatr. Clin. N. Am.* 42:1319–1341.

Belman, A.B. 1997. Vesicoureteral reflux. *Pediatr. Clin. N. Am.* 44:1171–1190.

Brisson, A., and R.H. Wade. 1983. Three-dimensional structure of luminal plasma membrane protein from urinary bladder. *J. Mol. Biol.* 166:21–36.

Chang, A., T.G. Hammond, T.-T. Sun, and M.L. Zeidel. 1994. Permeability properties of the mammalian bladder apical membrane. *Am. J. Physiol.* 267: C1483–C1492.

Chapman, C.J., R.R. Bailey, E.D. Janus, G.D. Abbott, and K.L. Lynn. 1985. Vesicoureteric reflux: segregation analysis. *Am. J. Med. Genet.* 20:577–584.

de Vargas, A., K. Evans, P. Ransley, A.R. Rosenberg, D. Rothwell, T. Sherwood, D.I. Williams, T.M. Barratt, and C.O. Carter. 1978. A family study of vesicoureteric reflux. *J. Med. Genet.* 15:85–96.

Devriendt, K., P. Groenen, H. Van Esch, M. van Dijck, W. Van de Ven, J.P. Fryns, and W. Proesmans. 1998. Vesico-ureteral reflux: a genetic condition? *Eur. J. Pediatr.* 157:265–271.

Dillon, M.J., and C.D. Goonasekera. 1998. Reflux nephropathy. *J. Am. Soc. Nephrol.* 9:2377–2383.

Eccles, M.R., R.R. Bailey, G.D. Abbott, and M.J. Sullivan. 1996. Unravelling the genetics of vesicoureteric reflux: a common familial disorder. *Hum. Mol. Genet.* 5:1425–1429.

Feather, S.A., S. Malcolm, A.S. Woolf, V. Wright, D. Blaydon, C.J. Reid, F.A. Flinter, W. Proesmans, K. Devriendt, J. Carter, P. Warwicker, T.H. Goodship, and J.A. Goodship. 2000. Primary, nonsyndromic vesicoureteric reflux and its nephropathy is genetically heterogeneous, with a locus on chromosome 1. *Am. J. Hum. Genet.* 66:1420–1425.

Finch, J.L., G.C. Webb, A. Evdokiou, and P.A. Cowled. 1997. Chromosomal localization of the human urothelial “tetraspan” gene, UPK1B, to 3q13.3-q21 and detection of a TaqI polymorphism. *Genomics.* 40:501–503.

Fukui, I., M. Yokokawa, G. Mitani, F. Ohwada, M. Wakui, M. Washizuka, T. Tohma, K. Igarashi, and T. Yamada. 1983. In vivo staining test with methylene blue for bladder cancer. *J. Urol.* 130:252–255.

Garin, E.H., A. Campos, and Y. Homsy. 1998. Primary vesicoureteral reflux: review of current concepts. *Pediatr. Nephrol.* 12:249–256.

Hicks, R.M. 1965. The fine structure of the transitional epithelium of rat ureter. *J. Cell Biol.* 26:25–48.

Hicks, R.M. 1975. The mammalian urinary bladder: an accommodating organ. *Biol. Rev. Camb. Philos. Soc.* 50:215–246.

Hicks, R.M., and B. Ketterer. 1969. Hexagonal lattice of subunits in the thick luminal membrane of the rat urinary bladder. *Nature.* 224:1304–1305.

Hiraoka, M., C. Hori, H. Tsukahara, K. Kasuga, Y. Ishihara, F. Kotsuji, and M. Mayumi. 1999. Vesicoureteral reflux in male and female neonates as detected by voiding ultrasonography. *Kidney Int.* 55:1486–1490.

Horowitz, M., A.B. Gershbein, and K.I. Glassberg. 1999. Vesicoureteral reflux in infants with prenatal hydronephrosis confirmed at birth: racial differences. *J. Urol.* 161:248–250.

Joyner, A.L. 1993. *Gene Targeting: A Practical Approach*. B.D. Hames, editor. Oxford University Press, Oxford, UK. 101–131.

Kachar, B., F. Liang, U. Lins, M. Ding, X.R. Wu, D. Stoffler, U. Aebi, and T.-T. Sun. 1999. Three-dimensional analysis of the 16 nm urothelial plaque particle: luminal surface exposure, preferential head-to-head interaction, and hinge formation. *J. Mol. Biol.* 285:595–608.

Kincaid-Smith, P.S., M.G. Bastos, and G.J. Becker. 1984. Relux nephropathy in the adult. *Contrib. Nephrol.* 39:94–99.

King, L.R. 1992. Vesicoureteral reflux, megaureter, and ureteral reimplantation. In *Campbell's Urology*. P.C. Walsh, A.B. Retik, E.D. Vaughan, Jr., and A.J. Wein, editors. W.B. Saunders & Co., Philadelphia, PA. 1689–1742.

Koss, L.G. 1969. The asymmetric unit membranes of the epithelium of the urinary bladder of the rat. An electron microscopic study of a mechanism of epithelial maturation and function. *Lab. Invest.* 21:154–168.

Lewis, S.A., and J.L. de Moura. 1982. Incorporation of cytoplasmic vesicles into apical membrane of mammalian urinary bladder epithelium. *Nature.* 297: 685–688.

Liang, F., B. Kachar, M. Ding, Z. Zhai, X.R. Wu, and T.-T. Sun. 1999. Urothelial hinge as a highly specialized membrane: detergent-insolubility, urohingin association, and in vitro formation. *Differentiation.* 65:59–69.

Lin, J.H., X.R. Wu, G. Kreibich, and T.-T. Sun. 1994. Precursor sequence, processing, and urothelium-specific expression of a major 15-kDa protein subunit of asymmetric unit membrane. *J. Biol. Chem.* 269:1775–1784.

Lyon, R.P., S. Marshall, and E.A. Tanagho. 1969. The ureteral orifice: its configuration and competency. *J. Urol.* 102:504–509.

Minsky, B.D., and F.J. Chlapowski. 1978. Morphometric analysis of the translocation of luminal membrane between cytoplasm and cell surface of transitional epithelial cells during the expansion-contraction cycles of mammalian urinary bladder. *J. Cell Biol.* 77:685–697.

Negrete, H.O., J.P. Lavelle, J. Berg, S.A. Lewis, and M.L. Zeidel. 1996. Permeability properties of the intact mammalian bladder epithelium. *Am. J. Physiol.* 271:F886–F894.

Nishimura, H., E. Yerkes, K. Hohenfellner, Y. Miyazaki, J. Ma, T.E. Hunley, H. Yoshida, T. Ichiki, D. Threadgill, J.A. Phillips III, et al. 1999. Role of the angiotensin type 2 receptor gene in congenital anomalies of the kidney and urinary tract, CAKUT, of mice and men. *Mol. Cell.* 3:1–10.

Noe, H.N., R.J. Wyatt, J.N. Peeden, Jr., and M.L. Rivas. 1992. The transmission of vesicoureteral reflux from parent to child. *J. Urol.* 148:1869–1871.

OMIM. 1999. *Online Mendelian Inheritance in Man*; Johns Hopkins University, Baltimore, MD; Vesicoureteral reflux; VUR; MIM Number 193000; Available online at: <http://www.ncbi.nlm.nih.gov/omim/>.

Peeden, J.N., Jr., and H.N. Noe. 1992. Is it practical to screen for familial vesicoureteral reflux within a private pediatric practice? *Pediatrics.* 89:758–760.

Pope, J.C. IV, J.W. Brock III, M.C. Adams, F.D. Stephens, and I. Ichikawa. 1999. How they begin and how they end: classic and new theories for the development and deterioration of congenital anomalies of the kidney and urinary tract, CAKUT. *J. Am. Soc. Nephrol.* 10:2018–2028.

Porter, K.R., and M.A. Bonneville. 1963. *The Fine Structure of Cells and Tissues*. Lea and Febiger, Philadelphia, PA. 116–117.

Ramirez-Solis, R., A.C. Davis, and A. Bradley. 1993. Gene targeting in embryonic stem cells. *Methods Enzymol.* 225:855–878.

Riedel, I., B. Czernobilsky, B. Lifschitz-Mercer, L.M. Roth, X.-R. Wu, T.-T. Sun, and R. Moll. 2000. Brenner tumors but not transitional cell carcinomas of the ovary show urothelial differentiation: immunohistochemical staining of urothelial markers, including cytokeratins and uroplakin III. *Virchows Archiv.* In press.

Roberts, J.A. 1992. Vesicoureteral reflux and pyelonephritis in the monkey: a review. *J. Urol.* 148:1721–1725.

Sant, G.R., and T.C. Theoharides. 1999. Interstitial cystitis. *Curr. Opin. Urol.* 9:297–302.

Shapiro, E., H. Lepor, and R.D. Jeffs. 1984. The inheritance of the exstrophy-epispadias complex. *J. Urol.* 132:308–310.

Smellie, J.M., and C. Normand. 1979. Reflux nephropathy in childhood. In *Reflux Nephropathy*. J. Hodson and P. Kincaid-Smith, editors. Masson Publishing, New York, NY. 14–20.

Stahelin, L.A., F.J. Chlapowski, and M.A. Bonneville. 1972. Luminal plasma membrane of the urinary bladder. I. Three-dimensional reconstruction from freeze-etch images. *J. Cell Biol.* 53:73–91.

Sun, T.-T., R. Eichner, D. Cooper, A. Schermer, W.G. Nelson, and R.A. Weiss. 1984. Classification, expression, and possible mechanisms of evolution of mammalian epithelial keratins: a unifying model. In *The Cancer Cell: The Transformed Phenotype*. Vol. 1. A. Levine, W. Topp, G. Vande Woude, and J.D. Watson, editors. Cold Spring Harbor Laboratory Press, Cold Spring Harbor, NY. 169–176.

Sun, T.-T., F.X. Liang, and X.R. Wu. 1999. Uroplakins as markers of urothelial

- differentiation. *Adv. Exp. Med. Biol.* 462:7–18.
- Surya, B., J. Yu, M. Manabe, and T.-T. Sun. 1990. Assessing the differentiation state of cultured bovine urothelial cells: elevated synthesis of stratification-related K5 and K6 keratins and persistent expression of uroplakin I. *J. Cell Sci.* 97:419–432.
- Tseng, S.C., M.J. Jarvinen, W.G. Nelson, J.W. Huang, M.J. Woodcock, and T.-T. Sun. 1982. Correlation of specific keratins with different types of epithelial differentiation: monoclonal antibody studies. *Cell.* 30:361–372.
- Vergara, J.A., W. Longley, and J.D. Robertson. 1969. A hexagonal arrangement of subunits in membrane of mouse urinary bladder. *J. Mol. Biol.* 46: 593–596.
- Walz, T., M. Haner, X.R. Wu, C. Henn, A. Engel, T.-T. Sun, and U. Aebi. 1995. Towards the molecular architecture of the asymmetric unit membrane of the mammalian urinary bladder epithelium: a closed “twisted ribbon” structure. *J. Mol. Biol.* 248:887–900.
- Wu, X.R., J.H. Lin, T. Walz, M. Haner, J. Yu, U. Aebi, and T.-T. Sun. 1994. Mammalian uroplakins. A group of highly conserved urothelial differentiation-related membrane proteins. *J. Biol. Chem.* 269:13716–13724.
- Wu, X.R., M. Manabe, J. Yu, and T.-T. Sun. 1990. Large scale purification and immunolocalization of bovine uroplakins I, II, and III. Mol markers of urothelial differentiation. *J. Biol. Chem.* 265:19170–19179.
- Wu, X.R., J.J. Medina, and T.-T. Sun. 1995. Selective interactions of UPIa and UPIb, two members of the transmembrane 4 superfamily, with distinct single transmembrane-domained proteins in differentiated urothelial cells. *J. Biol. Chem.* 270:29752–29759.
- Wu, X.R., and T.-T. Sun. 1993. Molecular cloning of a 47 kDa tissue-specific and differentiation-dependent urothelial cell surface glycoprotein. *J. Cell Sci.* 106:31–43.
- Yu, J., J.H. Lin, X.R. Wu, and T.-T. Sun. 1994. Uroplakins Ia and Ib, two major differentiation products of bladder epithelium, belong to a family of four transmembrane domain (4TM) proteins. *J. Cell Biol.* 125:171–182.
- Yu, J., M. Manabe, and T.-T. Sun. 1992. Identification of an 85-100 kDa glycoprotein as a cell surface marker for an advanced stage of urothelial differentiation: association with the inter-plaque (‘hinge’) area. *Epithelial Cell Biol.* 1:4–12.
- Yu, J., M. Manabe, X.R. Wu, C. Xu, B. Surya, and T.-T. Sun. 1990. Uroplakin I: a 27-kD protein associated with the asymmetric unit membrane of mammalian urothelium. *J. Cell Biol.* 111:1207–1216.